Građevinski materijali i konstrukcije
Building Materials and Structures
journal homepage: www.dimk.rs

https://doi.org/10.5937/GRMK2500002G

Original scientific paper

Numerical modelling of CFRP internally reinforced glulam beams

Ivan Glišović[1)], Marija Todorović[*1)], Nađa Simović[1)], Marko Pavlović[2)]

[1)] *Faculty of Civil Engineering, University of Belgrade, Belgrade, Serbia*
[2)] *Delft University of Technology, Delft,Netherlands*

Article history
Received: 03 March 2025
Received in revised form: 09 April 2025
Accepted: 14 April 2025
Available online: 15 May 2025

Keywords
Glulam,
CFRP plate,
FEM,
anisotropic plasticity,
progressive damage

ABSTRACT

Numerous studies have proven that timber structures can be effectively reinforced using fibre-reinforced polymer (FRP) composites. In this paper a nonlinear finite element model was developed to predict bending behaviour of glulam beams reinforced with carbon fibre reinforced polymer (CFRP) plates strategically located in the tension zone between the bottom two laminations. The developed model was validated through comparison with the results of experimental tests for both unreinforced and reinforced beams. To accurately simulate the mechanical behaviour of hybrid glulam-CFRP members, suitable constitutive relations for each material were utilised in the model. The theory of anisotropic plasticity was implemented to include plastic behaviour of timber laminations in the compression zone. The Hill's criterion for orthotropic materials was used as a condition for transition to the plastic state. The progressive damage model was introduced to effectively simulate softening behaviour of timber in tension. The FEM results have shown excellent agreement with the experimental results. Nonlinear behaviour of glulam beams internally reinforced with CFRP was achieved in the numerical analysis, demonstrating the accuracy of developed model past the linear-elastic range.

1 Introduction

Timber structures represent a popular choice in today's construction industry as a sustainable solution which has a positive impact on the environment and the experience of occupants. Accurate prediction of timber structural elements behaviour under different loading conditions is difficult due to variability in stiffness and strength properties of wood, which is a consequence of natural defects and discontinuities. Nowadays, there is an increasing tendency to eliminate those uncertainties and improve mechanical performance of timber structures. There are numerous studies proving the effectiveness of strengthening or reinforcing timber members using fibre-reinforced polymer (FRP) composites [1-9]. Features such as high stiffness and strength, low weight, good durability (no corrosion), electromagnetic neutrality, availability in different shapes and flexibility make FRP composites convenient for reinforcement of timber structures. FRP reinforcement placed in tension zone of timber beams may produce significant improvements in stiffness and ultimate load capacity. Two most commonly used FRPs are glass (GFRP) and carbon (CFRP).

As experimental research requires resources which make it a time-consuming and expensive, numerical models can be a time-saving and cost-effective solution. Additionally, numerical models can be used to further analyse and optimise existing experimentally obtained data. Some published works have already numerically investigated the performance of FRP-reinforced timber members in different arrangements. Nowak et al. [10] analysed CFRP strips inserted vertically and horizontally into the cross-section of timber beams by considering two behaviour models of wood: elastic and elastic-ideally plastic model. Although satisfactory agreement was obtained between experimental and numerical results, authors concluded that further research is needed in order to better describe the behaviour of timber beams under bending. Szczecina [11] studied glulam beams strengthened with CFRP plates in four-point bending test by considering different material models for timber (orthotropic linear-elastic and orthotropic elasto-plastic) and different definitions of cross-section of glulam beams (modelling of the whole section or division into laminations). FEM results showed that linear-elastic model is valid only for relatively small values of mid-span deflection and that division of cross-section into laminations has no significant impact. Raftery and Harte [12] discuss the development of a nonlinear finite element model that has the capability to predict the mechanical behaviour of low-grade glued laminated timber reinforced in flexure with GFRP plates. The model incorporates anisotropic plasticity theory for timber laminations in the compression zone of the glulam with the

* Corresponding author:
E-mail address: todorovicm@grf.bg.ac.rs

failure model based on the maximum stress criterion. Strong agreement is found between the simulated load-deflection behaviour and the experimental results of unreinforced and GFRP plate reinforced glulam. The model predicts the nonlinear performance of the reinforced beams with good accuracy with satisfactory results achieved in relation to elastic stiffness and ultimate moment capacity. Khelifa et al. [13] focused on the flexural behaviour of solid timber beams externally reinforced using CFRP. Elasto-plastic behaviour with damage effect was assumed for timber material. The conclusion was that the flexural behaviour of solid timber beams can be modelled through a local approach based on the coupling of orthotropic elasticity, Hill's plasticity anisotropic quadratic criterion and cohesive model.D. Harrach et al. [14] conducted reliability-based analysis by creating probabilistic nonlinear finite element models of glulam beams reinforced with CFRP plate as well as unreinforced glulam beam under bending. Properties of timber material are considered as random variables following a normal distribution with mean value and standard deviation. This research has successfully given a deep understanding of how uncertainties play a crucial role on the deformations and stresses of considered FE models. Based on these studies and results it has become clear that accurate definition of material behaviour is the most important part of modelling.

This paper presents numerical analysis of bending behaviour of glulam beams reinforced with CFRP plates strategically located in the tension zone between the bottom two laminations, performed with the aim of determining accurate stress-strain state. A nonlinear three-dimensional finite element model was developed using software package Abaqus.The theory of anisotropic plasticity was implemented to include plastic behaviour of timber laminations in the compression zone with the Hill's criterion for orthotropic materials as a condition for transition to the plastic state. Moreover, in order to improve existing FEM models, the progressive damage model was introduced to effectively simulate softening behaviour of timber in tension. Numerical model was validated through comparison of the predicted load-deflection behaviour, stiffness, maximum load and strain profile distribution with experimentally obtained data.

2 Materials and methods

2.1 Experimental research

The experimental testing was performed at the Laboratory of Structures, Faculty of Civil Engineering, University of Belgrade conducted the experimental testing. Eight unreinforced control glulam beams (Series A) and five glulam beams reinforced with CFRP plates incorporated in between two last laminations (Series F) were tested. These tests were a part of a larger study on reinforcement possibilities of glulam beams using FRP materials [6].

Geometry of the test series is shown in Fig. 1. Tested glulam beams were made from spruce timber classified in the strength class C24 according to EN 338 [15].Dimensions of glulam beams were 80 mm width × 210 mm height × 4000 mm length. Each beam was composed of seven 30 mm thick laminations. Reinforced beams were manufactured with six laminations, and the seventh one was added after the reinforcement was placed and proper bond was established between the reinforcement and the beam. Unidirectional CFRP plate (Sika CarboDur S613) was used as reinforcement with dimensions of 1.3 mm thickness × 60 mm width×4000 mm length. The manufacturer provided following mechanical properties: modulus of elasticity 165 GPa and tensile strength 2800 MPa [16]. The plate was bonded using epoxy adhesive (Sikadur-330). Bonded-in reinforcement is associated with improved fire protection, as well as being visually more acceptable in comparison to external reinforcement. In addition, the possibility of premature delamination is significantly reduced when reinforcement is placed internally due to a greater bond area [4].

Guidelines given in EN 408 [17] were followed during the testing in four-point bending configuration presented in Fig. 2. The beams were simply supported over 3780 mm span with the load applied in thirds of the span. Loading was stroke-controlled and it gradually increased until failure using a hydraulic jack. During testing, load was transformed from one load point to two load points using a steel beam. Roller bearings were used as supports and at the load application points. Steel plates were positioned at the load application and support positions to minimize the effects of local indentation. Moreover, lateral bracing was provided to prevent lateral instability of the beams. Load was recorded

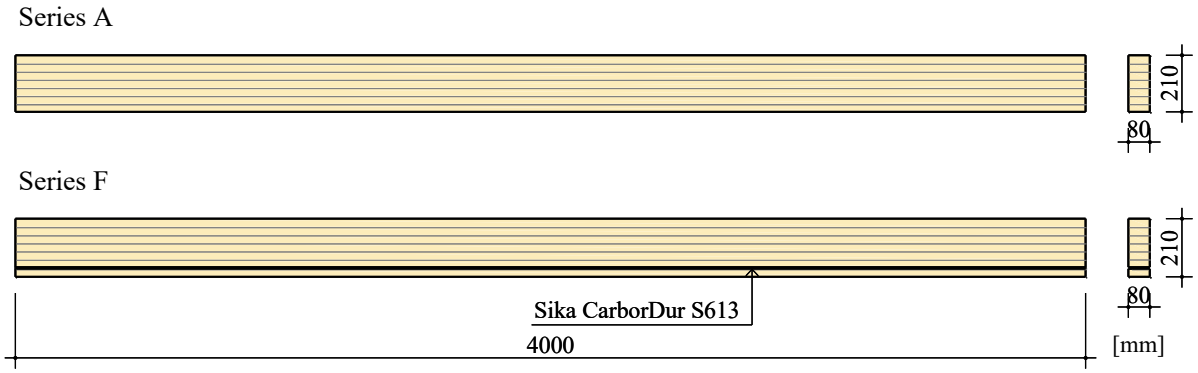

Fig. 1. Unreinforced (Series A) and reinforced beam (Series F)

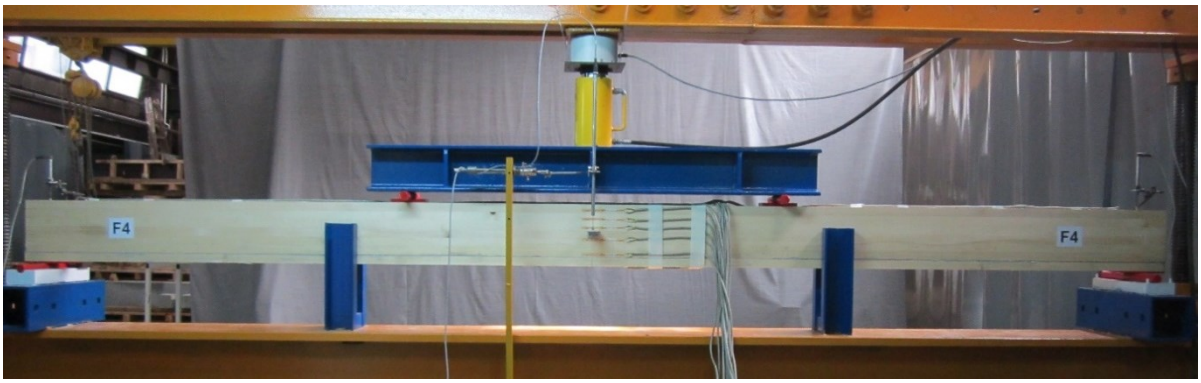

Fig. 2. Test layout

with a compression load cell, while deflection at mid-span was measured using linear variable differential transducers (LVDTs). Strains were measured using strain gauges at various locations throughout the beam's height at mid-span. All readings from loading cell, LVDTs and strain gauges were recorded using a computerized data acquisition system.

2.2 Numerical modelling

2.2.1 Model description

FEM software package Abaqus [18] was used for modelling of tested beams. As the experimental set-up was symmetrical around *x*- and *y*-axis, in order to optimize calculations, symmetry constraints were introduced and only 1/4 of the beam was modelled. The support was modelled as a roller bearing, restraining only the movement in vertical direction. Steel plates that were positioned at supports and loading points were also incorporated in the model to avoid stress concentrations at these sensitive positions. Based on experimental investigation, certain simplifications have been determined for the numerical model, such as:

– Each lamination was modelled separately to account for their different compressive and tensile behaviour, as explained in material characterisation chapter;

– Perfect connection was implemented at bonding interfaces between the laminations, since no bond-line failures were observed during experimental testing;

– A perfectly bonded connection was assumed to exist between timber and reinforcement as bonds of high quality were established during the experimental testing;

– No slip was included at the interface between steel plates and the timber surface.

Glulam beams were modelled using 8-node solid elements with reduced integration (C3D8R), CFRP plates using 4-node membrane elements with reduced integration (M3D4R) and steel plates using 4-node shell elements (S4), all available in Abaqus [18]. A mesh discretisation study was conducted to determine the finite element sizes. Two finite elements were adopted through the thickness of each timber lamination and one element through the thickness of CFRP plate. Finer mesh was generated for laminations adjacent to the CFRP plate, where stress transfer from CFRP plate to glulam occurs. Fig. 3 illustrates the adopted finite element mesh. The numerical analysis was performed using the Dynamic/Explicit solver. A series of vertical displacement increments were applied across the width of the beam until failure. As geometrical nonlinearities were considered, equilibrium equations are always formulated in the current configuration using current nodal positions, with the update of the finite element stiffness matrix at each increment [19].

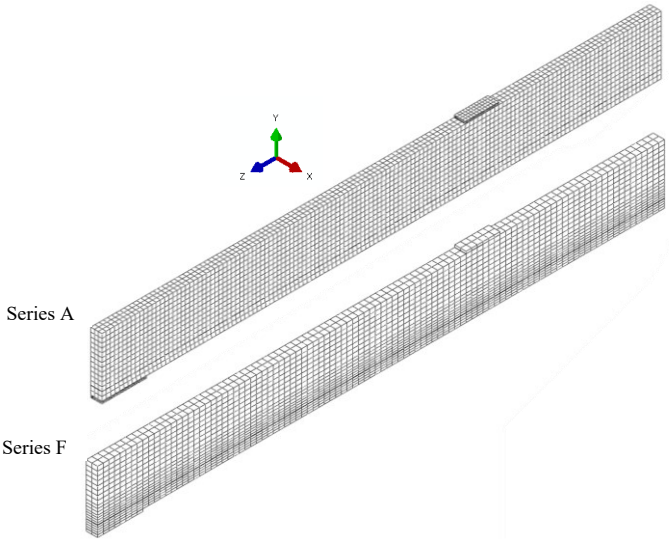

Fig. 3. Mesh discretisation for unreinforced (Series A) and reinforced (Series F) beams

2.2.2 Material characterisation

Accuracy of material modelling is of utmost importance in FEM modelling. Material input parameters for the finite element model were determined from material characterisation testing, known relationships and published data available in the constitutive relations for each material were utilised.

As timber is considered to be an orthotropic material, three main anatomical directions were assigned to the three principal axes (Fig.4).The behaviour of timber in the elastic region was described using nine independent engineering constants (three moduli of elasticity, three shear moduli and three Poisson's ratios).

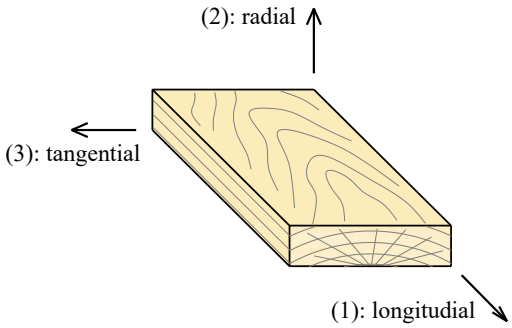

Fig. 4. Local coordinate system for timber

CFRP composite was considered to be a liner-elastic anisotropic material with transverse isotropy. Steel was treated as linear-elastic isotropic material.

Properties of each material were assumed to be independent of loading rates. Effects of environment, such as moisture and temperature, on the behaviour of timber were not taken into consideration. The material parameters of timber, CFRP plate and steel used for numerical simulations are presented in Table 1.

Table 1.Material parameters of timber and CFRP plates used in numerical modelling

	Timber	CFRP plate	Steel
Modulus of elasticity *E* (MPa)			
E_1	11,080	165,543	210,000
E_2	886	10,000	210,000
E_3	554	10,000	210,000
Poisson's ratio *v* (-)			
v_{12}	0.37	0.3	0.3
v_{13}	0.42	0.3	0.3
v_{23}	0.47	0.03	0.3
Shear modulus *G* (MPa)			
G_{12}	791	5,000	-
G_{13}	744	5,000	-
G_{23}	79	1,000	-

Experimental research was performed on small specimens to obtain the modulus of elasticity of timber (E_1) in the longitudinal direction. Timber has different moduli of elasticity for tension, compression and bending, but their values are very similar and for practical purposes assumed to be identical. General relationships as expressed in [20] were used to calculate the moduli in the transverse directions and shear planes, as well as Poisson's ratios. The elastic parameters for CFRP plate were adopted based on experimental tests (E_1) as well as values given in [21]. The properties in the plate thickness direction were taken the same as those in the transverse direction.

An important part of the numerical procedure is the selection of the most adequate timber strength values. Due to stress distribution effect in timber flexural members, tensile stress at failure is greater in bending than in axial tension. Hence, ultimate tensile stress was assumed to be equal to bending strength ($f_{t,0} = f_m$ =42.5 MPa) obtained from bending tests, which were conducted on small timber specimens taking into account size effect. The ultimate tensile stress will effectively be increased with addition of CFRP plate [6]. Horizontal reinforcement in tension zone acts as a bridge over timber defects and damages, and contributes to tensile capacity of the glulam beam. Experimental research has shown that the average extreme tensile strain at failure increased for reinforced over the unreinforced beams. Large strains at failure indicate large stresses at failure. Since no information was available for tensile strength in bending of reinforced timber, numerical procedure was modified to account for enhancement of bending strength using a modification factor. In this case, according to the ultimate tensile strain data, modification factor was taken as 1.25, therefore $f_{t,0,mod}$= 53 MPa.

Stress-strain relationship model for timber is presented in Fig. 5 where elastic-perfectly plastic behaviour was adopted for compression (negative part of the diagram) and elastic-softening behaviour for tension (positive part of the diagram).Exponential softening model was used to describe the softening behaviour of timber under tension [22]. Unmodified timber stress-strain curve was implemented for the bottom lamination. However, as the reinforcement influenced the laminations above it, modified stress-strain curve was adopted, as presented in Fig. 5.

Yield stresses of timber were considered to be equal to its compressive and shear strengths in various directions. These properties were estimated based onconducted material tests and available data for spruce timber in literature. The assumed yield points are shown in Table 2.

Table 2. Yield points assumed for numerical analysis

Yield stress (MPa)							
$\bar{\sigma}_{11}$	$\bar{\sigma}_{22}$	$\bar{\sigma}_{33}$	$\bar{\sigma}_{12}$	$\bar{\sigma}_{13}$	$\bar{\sigma}_{23}$	σ^0	τ^0
36.3	5.0	5.0	6.1	6.1	3.0	36.3	21.0

The theory of anisotropic plasticity was applied to include plastic mechanical behaviour of timber laminations in the compression zone. Plasticity was defined in Abaqus using yield stress and plastic strain. The Hill's criterion for orthotropic materials was used as a condition for transition to the plastic state:

$$f(\sigma)=\sqrt{F(\sigma_{22}-\sigma_{33})^2+G(\sigma_{33}-\sigma_{11})^2+H(\sigma_{11}-\sigma_{22})^2+2L\sigma_{23}^2+2M\sigma_{31}^2+2N\sigma_{12}^2} \quad (1)$$

where *F, G, H, L, M* and *N* are constants calculated based on the material strength characteristics for different directions:

$$F=\frac{(\sigma^0)^2}{2}\left(\frac{1}{\bar{\sigma}_{22}^2}+\frac{1}{\bar{\sigma}_{33}^2}-\frac{1}{\bar{\sigma}_{11}^2}\right)=\frac{1}{2}\left(\frac{1}{R_{22}^2}+\frac{1}{R_{33}^2}-\frac{1}{R_{11}^2}\right) \qquad L=\frac{3}{2}\left(\frac{\tau^0}{\bar{\sigma}_{23}^2}\right)^2=\frac{3}{2R_{23}^2}$$

$$G=\frac{(\sigma^0)^2}{2}\left(\frac{1}{\bar{\sigma}_{33}^2}+\frac{1}{\bar{\sigma}_{11}^2}-\frac{1}{\bar{\sigma}_{22}^2}\right)=\frac{1}{2}\left(\frac{1}{R_{33}^2}+\frac{1}{R_{11}^2}-\frac{1}{R_{22}^2}\right) \qquad M=\frac{3}{2}\left(\frac{\tau^0}{\bar{\sigma}_{13}^2}\right)^2=\frac{3}{2R_{13}^2} \tag{2}$$

$$H=\frac{(\sigma^0)^2}{2}\left(\frac{1}{\bar{\sigma}_{11}^2}+\frac{1}{\bar{\sigma}_{22}^2}-\frac{1}{\bar{\sigma}_{33}^2}\right)=\frac{1}{2}\left(\frac{1}{R_{11}^2}+\frac{1}{R_{22}^2}-\frac{1}{R_{33}^2}\right) \qquad N=\frac{3}{2}\left(\frac{\tau^0}{\bar{\sigma}_{12}^2}\right)^2=\frac{3}{2R_{12}^2}$$

Hill's parameters that were used in the model are:

$$R_{11}=\frac{\bar{\sigma}_{11}}{\sigma^0}=\frac{36.3}{36.3}=1 \qquad R_{12}=\frac{\bar{\sigma}_{12}}{\tau^0}=\frac{6.1}{21.0}=0.29$$

$$R_{22}=\frac{\bar{\sigma}_{22}}{\sigma^0}=\frac{5.0}{36.3}=0.14 \qquad R_{13}=\frac{\bar{\sigma}_{13}}{\tau^0}=\frac{6.1}{21.0}=0.29 \tag{3}$$

$$R_{33}=\frac{\bar{\sigma}_{33}}{\sigma^0}=\frac{5.0}{36.3}=0.14 \qquad R_{23}=\frac{\bar{\sigma}_{23}}{\tau^0}=\frac{3.0}{21.0}=0.14$$

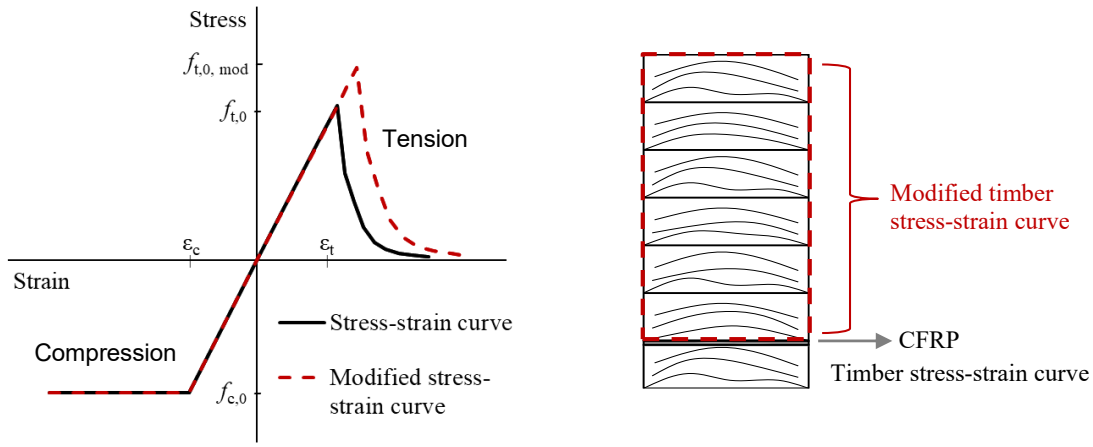

Fig. 5. Stress-strain curve for timber

For laminations in tension zone, the progressive damage model was introduced to effectively tackle the softening behaviour of timber. There are eight stress-based failure criteria or damage initiation functions proposed by Sandhaas and van de Kuilen[23]. Criterion I presents failure in tension parallel-to-grain, Criterion II –failure in compression parallel-to-grain, Criteria III–IV –failure in tension perpendicular-to-grain, Criteria V–VI– failure in compression perpendicular-to-grain and Criteria VII–VIII – shear failure. Failure Criterion I was selected to quantify damage initiation and propagation since tensile failure predominantly occurred in the experimental research. Additionally, only fracture due to tensile stress in the longitudinal direction of timber was considered. Therefore, softening behaviour and stiffness degradation in radial and tangential directions were neglected in order to optimize the calculations. The damage initiation and propagation criterion for failure in tension parallel-to-grain can be thus expressed as:

$$F_{t,0}(\sigma)=\sigma_L / f_{t,0} \le 1 \tag{4}$$

where σ_L– tensile stress parallel-to-grain of damaged material and $f_{t,0}$–tensile strength in bending.

Once a damage initiation criterion is satisfied, further loading will cause degradation of material stiffness coefficients. Reduction of stiffness coefficients is controlled by damage variables that have values between zero (undamaged state) and one (fully damaged state). Damage variable $d_{t,i}$ is expressed as:

$$d_{t,i}=1-\sigma_L / f_{t,0} \tag{5}$$

The evolution of each damage variable in the post-damage initiation phase is governed by an equivalent plastic displacement (Fig. 6). The equivalent plastic displacement for a failure mode is expressed as:

$$u_{pl}=L\,(\varepsilon_{pl}-\varepsilon_{0,pl}) \tag{6}$$

where ε_{pl}– strain of damaged material, $\varepsilon_{0,pl}$– strain at the onset of damage and *L*– characteristic length of the finite element.

Damaged material is implemented as a relation of damage variable *d* and equivalent plastic displacement u_{pl}, as shown in Fig. 6. Damage variable *d*is specified directly as a tabular function of equivalent plastic displacement u_{pl}, represented by a series of points on the diagram.

3 Results and discussion

Results obtained from the numerical model were verified through the comparison with the experimental test results. The global responses of the beams in terms of load versus mid-span deflection are shown in Fig. 7.

Linear load-deflection behaviour was recorded experimentally in the case of unreinforced glulam beams (Series A), as can be seen in Fig. 7. Failure was caused by excessive tensile stresses in bottom laminations. This failure mode is generally brittle and sudden without signs of compressive plasticization at the top. Failure was mostly initiated at defects or discontinuities (e.g. knots), which were located in the zone of maximum bending moment between load application points. Behaviour predicted by the finite element model for unreinforced beams was entirely linear elastic up to failure and demonstrates good agreement with experimentally determined behaviour.

Glulam beams reinforced with CFRP plate (Series F) demonstrated significant nonlinear load-deflection behaviour (Fig. 7). The most frequent failure mechanism of these beams included two stages: local failure at timber lamination below the reinforcement and global failure above the reinforcement. After the initial linear-elastic behaviour, load resistance decreased sharply due to tensile/bending failure of the bottom lamination below the reinforcement (evident as a sudden drop in the load-deflection curve). As the reinforcement remained in position, the beams continued to carry the load in the same way as beams reinforced at the intrados surface (with reduced cross-section and increased reinforcement percentage) which resulted in nonlinear load-deflection behaviour. Load increased up to a subsequent global tensile/bending failure in laminations above the CFRP plate. Failure in the tension zone was accompanied by pronounced shear cracks that extended along the timber-reinforcement interface and/or through timber laminations above the reinforcement (Fig. 8a). Compression wrinkles were clearly visible in the top laminations, but the failure did not occur in the compression zone (Fig. 8b). Horizontal shear failure after partial cracking of timber lamination below the reinforcement. It was caused by a wood defect that manifests as tangential separation of the wood fibres along parts of the annual rings (ring shake). In addition, one beam had a premature tension failure initiated in the lamination above the reinforcement caused by a large knot. Due to the brittle nature of the timber's behaviour in tension and shear, these two beams failed suddenly, without visible warning signs before reaching ultimate load carrying capacity. The influence of different failure mechanisms of reinforced beams on the deflection values is significantly higher than on the maximum load values. The effectiveness of the reinforcement is mainly conditioned by the wood defects. A higher degree of reinforcement activation introduces nonlinearity into the global behaviour of the beams and enables less brittle failure compared to the unreinforced beams.

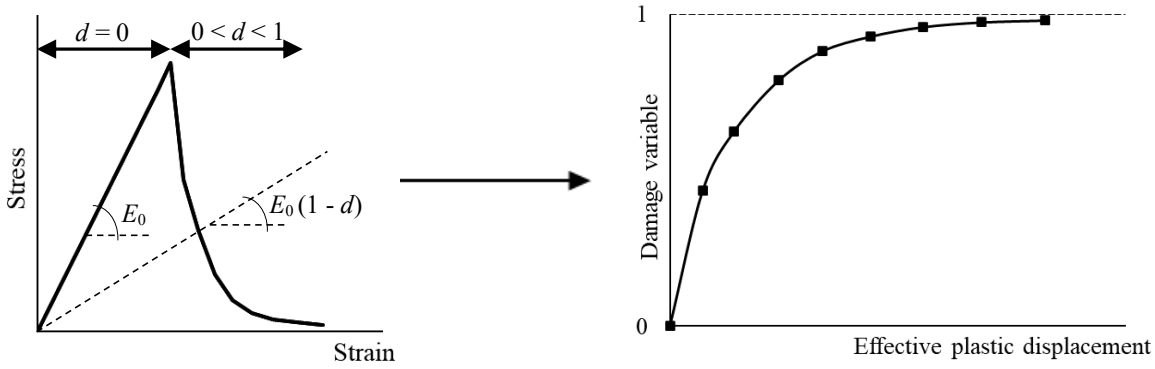

Fig. 6. Stress-strain curve transformation to damage variable-effective plastic displacement

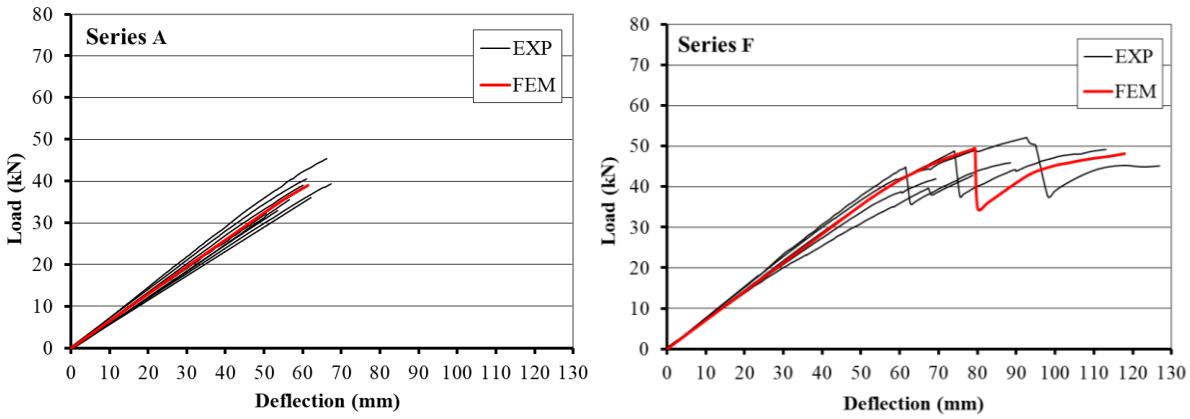

Fig. 7. Load-deflection curves for unreinforced (Series A) and reinforced (Series F) beams

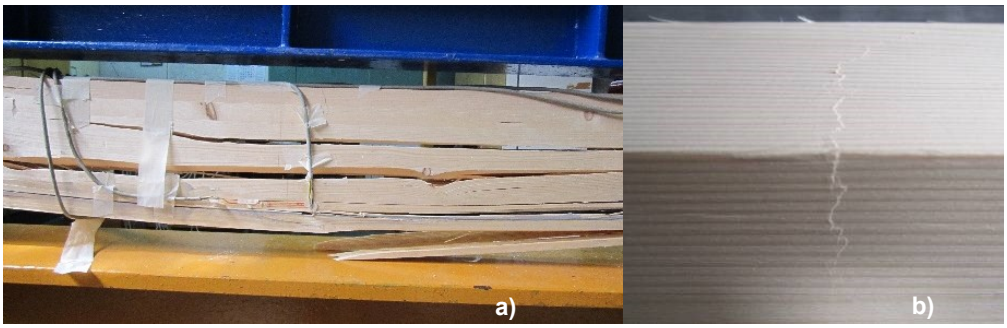

Fig. 8. Failure mode of reinforced beams: a) global tensile failure in laminations above CFRP plate; b) compression wrinkles in top laminations

FEM model of reinforced beams replicated the behaviour of experimentally tested specimens, including the failure in two stages: local failure in the timber lamination below the CFRP plate and global failure in the timber lamination above the CFRP plate. Once the first stage failure happened, the bottom lamination was excluded from the further analysis and rest of the beam continued carrying the load until the global failure. Nonlinear behaviour of beams before global failure was recorded in the numerical model, confirming the FEM model to be accurate past the linear-elastic range.

The normal stress distributions in the reinforced beam obtained from the numerical analysis are given in Figs. 9a and 10a.The area of maximum stresses, which corresponds to the bending moment diagram, can be clearly seen. In the first stage (before the failure of the timber lamination below the reinforcement), the distribution of normal stresses is almost identical in the tension and compression zones. The normal stresses increase with distance from the cross-section's centre of gravity, with the maximum normal stress occurring at the soffit of the beam. The tensile fracture in the lamination below the CFRP platewas determined by the local deformation in the area under the steel plate where the load was applied. Due to the plasticization of the compression zone, within the second stage (after the failure of the timber lamination below the reinforcement), distribution of normal stresses is not uniform. Reaching the ultimate tensile stress in the timber lamination above the reinforcement leads to the global failure of the reinforced beam.

The normal stress distributions in the CFRP plate of the reinforced beam are uniform along the entire length, as seen in Figs. 9b and 10b.The results of the numerical analysis show that the plate capacity is generally underutilized in the linear region of the beam's behaviour (first stage). After the plasticization in the compression zone (second stage), the degree of CFRP plate utilization is somewhat higher. The calculated maximum tensile stress in the plate at the ultimate load of reinforced beam was less than 40% of its tensile strength.

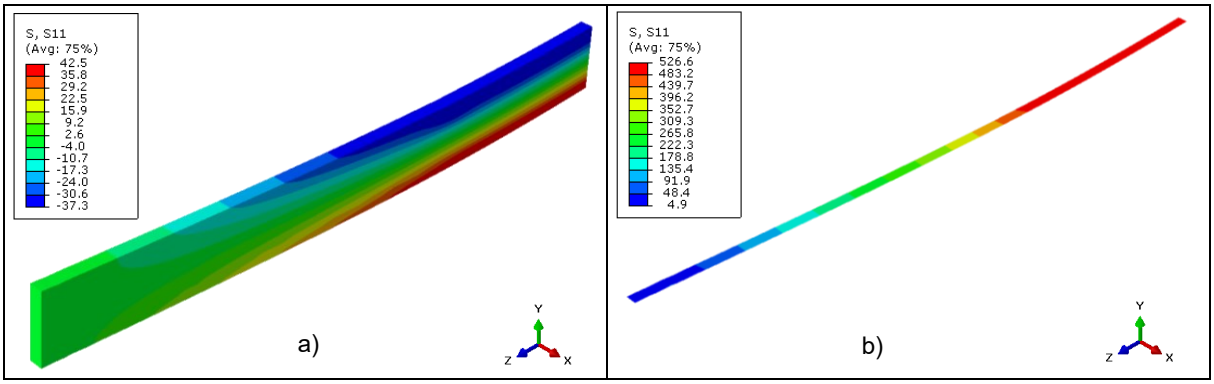

Fig. 9. Tensile stress σ_{11} (MPa) atthe moment of local failure of the reinforced beam: a) in glulam; b) in CFRP plate

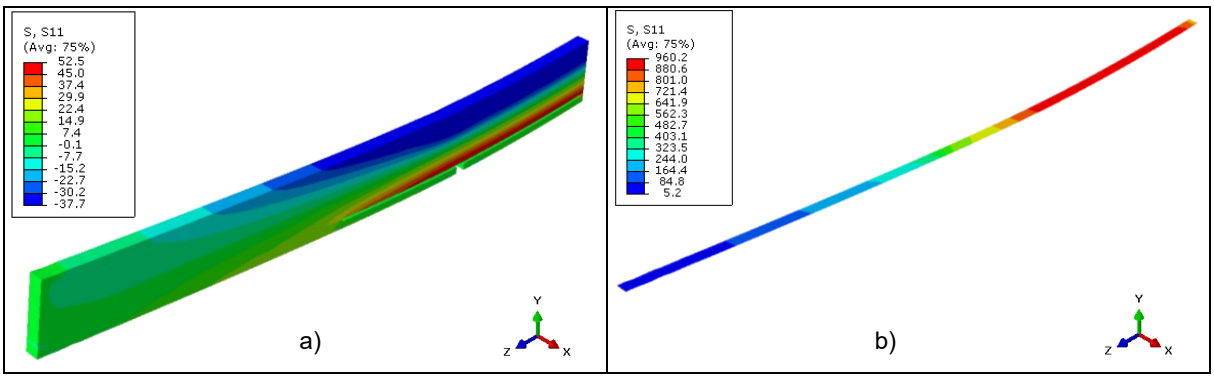

Fig. 10. Tensile stress σ_{11} (MPa) at the moment of global failure of the reinforced beam: a) in glulam; b) in CFRP plate

The results of experimental tests and numerical modelling in regard to ultimate load capacity, mid-span deflection at failure, and elastic bending stiffness, are summarized in Table 3. The effect of reinforcement on the ultimate load-carrying capacity, stiffness and deformability is clearly demonstrated. The last column compares the model's results with the average experimental results.

Table 3. Experimental and numerical results

Test series	Exp.	FEM	FEM/Exp. (%)
Maximum load (kN)			
Series A	37.9 (CV = 12.1 %)	39.0	2.9
Series F	46.4 (CV = 9.3 %)	47.6	2.7
Maximum mid-span deflection (mm)			
Series A	59.9 (CV = 10.0 %)	61.7	3.0
Series F	95.3 (CV = 25.2 %)	113.9	19.5
Bending stiffness *EI* (× 10^{11} Nmm^2)			
Series A	6.46 (CV = 7.7 %)	6.53	1.1
Series F	7.28 (CV = 6.2 %)	7.12	–2.2

CV – Coefficient of variation

Numerical and experimental values of load-carrying capacity are very close with a difference of approximately 3% for both unreinforced and reinforced beams. In both cases, the predicted value of the maximum load was higher than the experimental value. It was anticipated that the results would differ even more when knots and other timber defects were taken into account.

The FE model predicted stiffness values agree well with those experimentally determined, with differences of about 2%. This small deviation proves the uniform quality of the laminations. Given that agreement is strong, it is confirmed that the assumption of perfect adhesion between the CFRP and timber is valid.

The mid-span deflection values show satisfactory compatibility for unreinforced beams. However, the numerical and experimental values of the mid-span deflection at failure show a noticeable difference of about 20% for Series F. The cause of this deviation is variability in the experimentally recorded fracture patterns of the beams. If two reinforced beams, which did not have characteristic failure mechanisms in two stages, are omitted from the experimental analysis (premature tensile failure – Beam F2 and shear failure – Beam F3), the obtained numerical value of deflection is lower than the experimental one, with better agreement of results (difference of 4.0%).

Fig. 11 illustrates the comparisons of experimental and numerical strain profiles at mid-span for different load levels.Strain distribution in mid-span across the height was linear until failure in the case of unreinforced beams. Tensile and compressive strains were almost identical at different load levels. The position of the neutral axis remained unchanged as the load increased, which proved there was no plasticization in the compression zone.

For the reinforced beams linear strain distribution across the height was observed in the elastic region. Neutral axis moved towards tension zone due to contribution of the CFRP plate. After failure of bottom lamination, neutral axis shifted upwards. No significant variation of neutral axis position was recorded as the applied load increased and plasticization in compression zone occurred. A non-linear strain distribution prior to global failure was noticed. In addition to improvement in tension strains, strain results demonstrated that timber compressive properties were better utilized when CFRP reinforcement was included in the tension zone.

Good agreement of the results is achieved from the simulated strain profiles for both sets of beams. The difference that exists between numerical predictions and experimental values is a result of an average timber modulus of elasticity being used for each lamination, when actually each lamination is inhomogeneous and material properties of timber vary throughout. Also, the reason for deviations in the nonlinear region can be explained by the assumption in the numerical analysis that plane sections remain plane after plastic deformation.

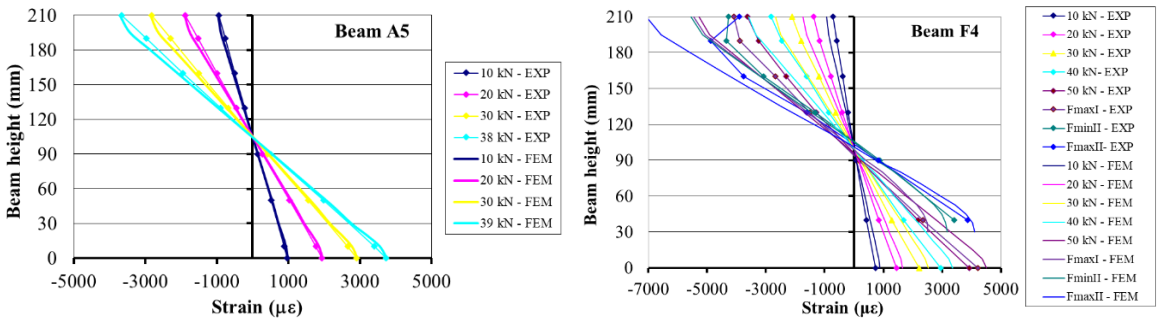

Fig. 11. Strain profiles at different load levels for unreinforced (Series A) and reinforced (Series F) beams

5 Conclusions

The effectiveness of FRP reinforcement of timber members has been proven through various studies.In order to better understand mechanical performance of CFRP plate reinforced glulam beams, a nonlinear finite element model was developed. Finite element modelling approach implemented in this paper was based on elasto-plastic and orthotropic characteristics of timber, Hill's plasticity criterion and progressive damage model to account for softening behaviour of timber in tension. Numerical predictions confirmed previousexperimental research.

Proposed FE models simulated experimentally obtained load-deflection curves and failure modes for both unreinforced and reinforced glulam beams. Numerical model demonstrated linear load-deflection behaviour and brittle tensile failure in bottom laminations of unreinforced beams. Predicted model for reinforced beams replicated failure in two stages:local failure of timber lamination below the reinforcement and global failure of the beam above the reinforcement, with significant nonlinear load-deflection behaviour. The progressive damage modelling has the ability to predict nonlinear response of reinforced beams accurately.

Good agreement between numerical and experimental data was found for bending stiffness, ultimate load-carrying capacity and mid-span deflection at failure. Numerical results demonstrated that adding the CFRP plate in the tension zone of the section improved the ultimate load-carrying capacity, stiffness and ductility of glulam beams. Furthermore, the strain profile distributions predicted by the FE models agreed well with the experimental findings. The assumption of plane sections is acceptable for glulam beams reinforced with CFRP composites.

The proposed numerical approach proved to be helpful in analysing test results and improving comprehension of stress and deformation states in timber and reinforcement. The developed model is easily adjustable to different loading configurations, beam dimensions and material properties. Therefore, it is a valuable tool that can be used to optimise the design of timber beams reinforced with FRP plates, including determination of optimal reinforcement percentage and arrangement.

CRediT authorship contribution statement

Ivan Glišović: Conceptualization, Investigation, Formal analysis, Supervision, Writing – review & editing.

Marija Todorović: Conceptualization, Methodology, Software, Writing – original draft

Nađa Simović: Writing – review & editing, Software.

Marko Pavlović:Methodology, Software.

Declaration of competing interest

The authors declare that they have no known competing financial interests or personal relationships that could have appeared to influence the work reported in this paper.

Acknowledgement

This research was supported by the Science Fund of the Republic of Serbia, Serbian Science and Diaspora Collaboration Program: Knowledge Exchange Vouchers: Hybrid structures and connection of timber and FRP.

References

[1] J. Fiorelli, A.A. Dias, Glulam beams reinforced with FRP externally bonded: Theoretical and experimental evaluation. Materials and Structures 44(8) (2011) 1431-1440. https://doi.org/10.1617/s11527-011-9708-y.

[2] G.M. Raftery, A.M. Harte, Low-grade glued laminated timber reinforced with FRP plate. Composites: Part B 42(4) (2011) 724-735. http://dx.doi.org/10.1016/j.compositesb.2011.01.029.

[3] Y.J. Kim, M. Hossain, K.A. Harries, CFRP strengthening of timber beams recovered from a 32 year old Quonset: Element and system level tests. Engineering Structures57 (2013) 213-221.https://doi.org/10.1016/j.engstruct.2013.09.028.

[4] G.M. Raftery, C. Whelan, Low-grade glued laminated timber beams reinforced using improved arrangements of bonded-in GFRP rods. Construction and Building Materials52 (2014) 209-220. https://doi.org/10.1016/j.conbuildmat.2013.11.044.

[5] A. D'Ambrisi, F. Focacci, R. Luciano, Experimental investigation on flexural behaviorof timber beams repaired with CFRP plates. Composite Structures 108 (2014) 720-728. https://doi.org/10.1016/j.compstruct.2013.10.005

[6] I. Glišović, B. Stevanović, M. Todorović, Flexural reinforcement of glulam beams with CFRP plates. Materials and Structures 49(7) (2016) 2841-2855. https://doi.org/10.1617/s11527-015-0690-7

[7] H. Yang, W. Lin, W. Lu, S. Zhu, O.Geng, Flexural behaviour of FRP and steel reinforced glulam beams: Experimental and theoretical evaluation. Construction and Building Materials 106 (2016) 550-563. https://doi.org/10.1016/j.conbuildmat.2015.12.135

[8] B. Kasal, L. Yan, Fibre-reinforced polymers as reinforcement for timber structural elements,in: J. Branco, P. Dietsch, T. Tannert (Eds.), Reinforcement of timber elements in existing structures, State-of-the-Art Report of the RILEM TC 245-RTE, Springer, 2021, pp. 51–78.

[9] M. Todorović, I. Glišović, B. Stevanović, Experimental investigation of end-notched glulam beams reinforced with GFRP bars. European Journal of Wood and Wood Products 80(5) (2022) 1071-1085. https://doi.org/10.1007/s00107-022-01822-6

[10] T.P. Nowak, J. Jasienko, D. Czepizak, Experimental tests and numerical analysis of historic bent timber elements reinforced with CFRP strips. Construction and Building Materials 40 (2013) 197-206.https://doi.org/10.1016/j.conbuildmat.2012.09.106

[11] M. Szczecina, Study of Complexity of Numerical Models of a Strengthened Timber Beam. Materials 16 (2023) 3466.https://doi.org/10.3390/ma16093466

[12] G.M. Raftery, A.M. Harte, Nonlinear numerical modelling of FRP reinforced glued laminated timber. Composites: Part B 52 (2013) 40-50. https://doi.org/10.1016/j.compositesb.2013.03.038

[13] M. Khelifa, S. Auchet, P.J. Meausoone, A. Celzard A, Finite element analysis of flexural strengthening of timber beams with carbon fibre reinforced polymers. Engineering Structures 101 (2015) 364-375. https://doi.org/10.1016/j.engstruct.2015.07.046

[14] rach, H. Muayad, R. Majid Movahedi, Reliability-based numerical analysis of glulam beams reinforced with CFRP plate. Scientific Reports 12 (2022) 13587.https://doi.org/10.1038/s41598-022-17751-6

[15] EN 338: Structural timber - Strength classes, European Committee for Standardization, Brussels, Belgium, 2009.

[16] Sika CarboDur plates: Pultruded carbon fibre plates for structural strengthening, 2015. Product Data Sheet, Sika AG, 2015.

[17] EN 408: Timber structures - Structural timber and glued laminated timber - Determination of some physical and mechanical properties, European Committee for Standardization, Brussels, Belgium, 2010.

[18] Abaqus/CAE. User's Guide, Version 2017; Dassault Systems Simulia Corp: Johnston, RI, USA, 2016.

[19] R.D.S.G. Campilho, M.F.S.F. de Moura, A.M.J.P. Berreto, J.J.L. Morais, J.J.M.S. Domingues, Fracture behaviour of damaged wood beams repaired with an adhesively-bonded composite patch. Composites: Part A 40 (2009) 852-859. https://doi.org/10.1016/j.compositesa.2009.04.007

[20] J. Bodig, B.A. Jayne, Mechanics of wood and wood composites. Van Nostrand Reinhold Company, New York, 1982.

[21] B. Harris, Engineering composite materials. The Institute of Materials, London, 1999.

[22] M. Wang, X. Song, X. Gu, Three-dimensional combined elastic-plastic and damage model for nonlinear analysis of wood. Journal of Structural Engineering 144(8) (2018) 04018103.https://doi.org/10.1061/(ASCE)ST.1943-541X.0002098

[23] C. Sandhaas, J.W.G. van de Kuilen, Material model for wood. HERON 58(2/3), 2013.